European Journal of Orthodontics 31 (2009) 221–231
doi:10.1093/ejo/cjp032

Induction of osteopenia during experimental tooth movement in the rat: alveolar bone remodelling and the mechanostat theory

Trudy J. Milne*, Ionut Ichim*, Bhavik Patel*, Andrew McNaughton** and Murray C. Meikle*,***

*Faculty of Dentistry, **Department of Anatomy and Structural Biology, University of Otago, New Zealand and ***Faculty of Dentistry, National University of Singapore, Singapore

SUMMARY Increases in bone strains above a certain threshold have a positive effect on bone mass, whereas reductions in strain magnitude lead to bone loss and osteopenia; the term 'mechanostat' has been introduced to describe this tissue-level negative feedback mechanism. The mechanobiology of bone and particularly alveolar bone is poorly understood, and whether the mechanostat theory has any relevance to explaining the osseous changes that occur during orthodontic tooth movement remains unclear. To investigate the relationship further, an expansile force of 0.2 N was applied to the maxillary molars of 36, 6-week-old Wistar rats by helical coil springs. The animals were sacrificed at 1, 2, 4, and 8 days and the tissue response analyzed by histological, biochemical, and finite element (FE) methods. Differences between groups were determined by Student's *t*-test (two-tailed).

The appliance produced an increase in the intermolar width averaging 0.5 mm after 8 days. Tetracycline uptake in the control rats suggested a rapid turnover of bone in both the interradicular domain and the bone–periodontal ligament interface. In the experimental group, however, incorporation of tetracycline into the interradicular domain was reduced and conventional histology revealed evidence of bone loss and osteopenia, in both the experimental and a group of sham-treated positive controls (with inactive, annealed springs). Serum alkaline phosphatase declined significantly in both experimental and sham-treated groups over the 8-day time course, indicating decreased bone formation. Serum acid phosphatase also declined, suggesting a concomitant decrease in bone resorption. Three-dimensional FE analysis of the stresses generated in the bone following occlusal (2 N) and orthodontic loading showed that the orthodontic force created a constant loading condition shielding some areas of bone from mechanical stress. Areas of low mechanical stimulation were coincident with sites of bone loss observed histologically, while bone mass was preserved in areas with higher levels of loading.

These findings suggest that (1) the osteopenia resulted from stress shielding of the interradicular bone by the appliance, and a consequent reduction in occlusal loading below the critical threshold required for maintaining normal osseous architecture and (2) the mechanostat model can be employed to explain, at least in part, the response of the bone to orthodontic loading.

Introduction

The correction of malocclusion is dependent upon the capacity of the tissues of the periodontium to react to changes in their mechanical environment. The current view is that the forces orthodontic appliances apply to the teeth are transmitted through the periodontal ligament (PDL) to the supporting alveolar bone, leading to deposition or resorption, depending upon whether the tissues are exposed to a tensile or compressive mechanical strain (Meikle, 2006).

Mechanical function is an important determinant of bone mass and architecture. Increases in bone strains above a certain threshold resulting from physical activity have a positive effect on bone mass (Nilsson and Westlin, 1971; Jacobson *et al.*, 1984) that does not require a prior episode of bone resorption (Lanyon and Baggott, 1976; Chow *et al.*, 1998). Reductions in strain magnitude on the other hand resulting from weightlessness or prolonged bed rest lead to bone loss and osteopenia (Donaldson *et al.*, 1970; Jee *et al.*, 1983). Furthermore, stress shielding and osteopenia resulting from the implantation of rigid metallic devices into bone is a well-recognized complication of total hip arthroplasty and fracture fixation in orthopaedic surgery (Huiskes *et al.*, 1992; Glassman *et al.*, 2006). The term 'mechanostat' was introduced by Frost (1987) to describe this tissue-level negative feedback mechanism. Although the single-word terminology adopted (modelling for increases in bone mass; remodelling for bone loss) can be confusing to those for whom the definition of remodelling includes resorption and formation, it has proved useful to describe the complexity of the skeletal response to mechanical loading and led to a wider appreciation of how bones adapt to their functional environment (Skerry, 2006).

Most *in vivo* studies of orthodontic tooth movement have concentrated on changes occurring within the PDL.

However, the PDL can only provide a partial explanation for the mechanisms involved in dentoalveolar remodelling, and more attention has focused lately on the wider response of the alveolar bone (Melsen, 1999, 2001; Verna *et al.*, 1999; Pavlin *et al.*, 2001). Recent proposals have suggested that orthodontic loading may trigger bone remodelling by producing microdamage (Verna *et al.*, 2004) or by stimulating the induction of a regional acceleratory phenomenon (Melsen, 1999; Verna *et al.*, 1999)—a reaction to trauma in which the rate of bone remodelling exceeds normal tissue activity.

In the present study, preliminary histological and biochemical findings from a rat model in which the maxillary molars were moved buccally with a palatal expansion spring are described. For the first time, it was observed that insertion of an orthodontic appliance was accompanied by bone loss and osteopenia of the interradicular bone. To resolve the question whether the osteopenia resulted from stress shielding of the bone by the appliance, a three-dimensional finite element (3D FE) analysis of the stresses generated in the PDL and alveolar bone under conditions of both orthodontic and occlusal loading was carried out.

Material and methods

The 74, 6-week-old male Wistar rats used in this study were housed at the Hercus Taieri Resource Unit at the University of Otago Medical School under standard laboratory conditions and fed powdered rat chow (R94, Reliance Stock Feeds, Dunedin, New Zealand) and water *ad libitum*. Ethical approval for all experimental procedures was obtained from the University of Otago Animal Ethics Committee and undertaken in accordance with the International Guiding Principles for Animal Research.

Appliance insertion

The animals were anaesthetized with a subcutaneous mixture of Ketamine (Ketamine hydrochloride; 75 mg/kg body weight) and Domitor® (Medetomidine hydrochloride, 0.5 mg/kg body weight; Pfizer New Zealand, Auckland, New Zealand). Standardized helical coil springs designed to move the molar teeth buccally were constructed from 0.012 inch stainless steel wire (Premium Plus; A J Wilcock, TP Orthodontics, La Porte, Indiana, USA) on a brass jig and bonded to the palatal surfaces of the maxillary first and second molars (Figure 1A) using Transbond Plus Self Etching Primer (3M Unitek, Monrovia, California, USA) and light-activated composite resin (Filtek Flow; 3M-Espe, Auckland, New Zealand). The springs were activated to deliver a force of 0.2 N; anaesthesia was reversed with Antisedan (Atipamezole hydrochloride, 0.5 mg/kg body weight; Pfizer New Zealand).

Hard tissue specimens

In the first experimental series, 28 animals (four experimental and three negative controls at each time point) were killed in a carbon dioxide chamber after 1, 2, 4, and 8 days and the heads fixed in 10 per cent neutral buffered formalin at 4°C. Each animal received a subcutaneous injection of tetracycline hydrochloride (T 3383; Sigma-Aldrich, Auckland, New Zealand; 30 mg/kg body weight) dissolved in 0.9 per cent sodium chloride, 24 hours prior to sacrifice.

These specimens were used to (1) measure the amount of tooth movement between the mesio-buccal grooves of the maxillary first molars (to 0.01 mm) with a Nikon Measurescope (Nikon Corporation, Tokyo, Japan) linked to a Sony video monitor (Sony Corporation, Tokyo, Japan) and Nikon digital counter (CM-66) and (2) identify sites of new

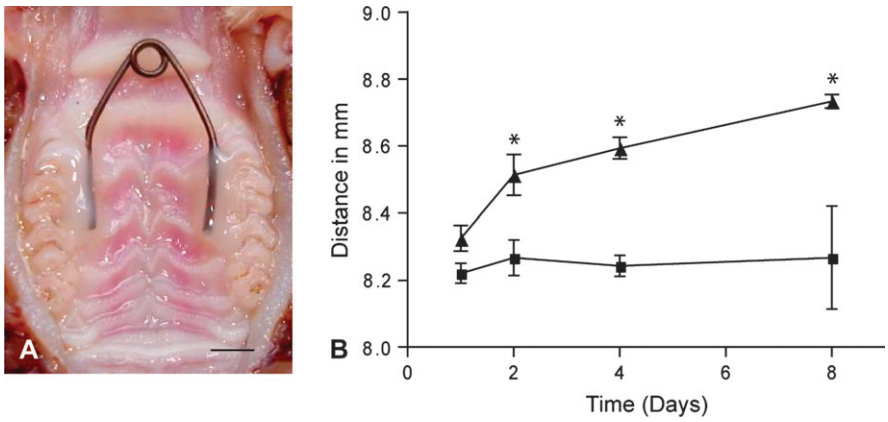

Figure 1 (A) Stainless steel helical coil spring (0.012 inch) bonded to the maxillary first and second molars of a 6-week-old Wistar rat and calibrated to deliver an expansile force of 0.2 N (approximately 20 g). Bar = 2.0 mm. (B) Increase in intermolar width (mean ± standard error of the mean) measured from the mesio-buccal groove of M1 to M1 (3 control; 4 experimental rats at each point in the timescale). ▲, experimental; ■, control. *Significantly different from controls. $P < 0.05$.

bone formation. The upper jaws were dehydrated in a graded series of ethanols and embedded in polymethylmethacrylate. Sections were cut parallel to the occlusal plane with a diamond disc in an IsoMet® Low Speed Saw (Buehler Ltd, Lake Bluff, Illinois, USA) and further reduced to 100–150 μm in a Phoenix Beta polishing machine (Buehler Ltd). The sections were mounted in Vectashield Mounting Medium (Vector Laboratories, Burlingame, California, USA) to minimize photobleaching, and viewed by ultraviolet fluorescent microscopy with a Nikon Eclipse 80i microscope (Nikon Corporation).

Decalcified specimen preparation

The aim of the second experimental series was to provide histological detail not achievable with tetracycline-labelled sections. To determine the potential effect of the appliance itself, a positive control (sham) group of animals was included with softened, passive springs that had been annealed by heating to a high temperature. Forty-six animals in total were euthanized at zero time ($n = 6$) and 1, 2, 4, and 8 days (five experimental and five positive controls at each time point). The upper jaws were removed, fixed in Histochoice™ MB© Fixative (Amresco Inc., Bio-Strategy, Albany, New Zealand) at 4°C overnight and decalcified with 10 per cent ethylenediaminetetraacetic acid in phosphate buffered saline (PBS) at 4°C for 3–4 weeks. Following decalcification, the specimens were rinsed in diethyl pyrocarbonate-treated PBS twice for 1 minute and dehydrated in a graded series of ethanols. The molar teeth and supporting alveolar bone were dissected free, divided along the mid-palatal suture, and each hemi-maxilla embedded in paraffin wax; horizontal sections from one hemi-maxilla were cut at 5 μm, and every 10th section stained with haematoxylin and eosin.

Serum measurements

At sacrifice, blood was collected by cardiac puncture after thoracotomy into glass tubes and allowed to coagulate for 30 minutes on ice. After centrifugation at ×3000 *g* for 20 minutes at 4°C, the serum was transferred to new tubes and frozen at −20°C. Alkaline phosphatase (ALP) and acid phosphatase (ACP) activity were measured using *p*-nitrophenol phosphate (*p*NPP) as substrate (BioAssay Systems, Hayward, California, USA); *p*-NPP for constructing standard curves was obtained from Sigma-Aldrich. For ALP, an assay buffer containing 100 mM Tris-HCl, pH 8.6 with 10 mM $MgCl_2$ was used and absorbance was measured at 405 nm. For ACP, the assay buffer contained 100 mM sodium acetate, pH 5.5 with 10 mM $MgCl_2$; absorbance was measured at 405 nm. The data set was based on serum samples from five animals at each time point assayed in triplicate. One unit of *p*NPP activity is defined as 1 μmol of *p*-NPP liberated per minute at 37°C (1 unit = μmol/l/min).

Interleukin-1β (IL-1β) and Interleukin-6 (IL-6) were measured in serum samples by Quantikine® colorimetric sandwich enzyme-linked immunosorbent assays (ELISAs) specific for the rat proteins (R&D Systems; Pharmaco Ltd, Auckland, New Zealand).

Statistical methods

Data were expressed as the mean ± standard error of the mean (SEM). Differences between groups were determined by Student's *t*-test (two-tailed) using GraphPad Prism (GraphPad Software Inc., San Diego, California, USA) and the level of significance set at $P < 0.05$.

3D FE analysis

3D FE analysis was used to evaluate the stresses and strains developed in the maxilla under both orthodontic and masticatory loading. The skull of a 6-week-old control rat was scanned by X-ray microcomputed tomography (CT) using a SkyScan 1072 desktop micro-CT scanner (SkyScan, Aartselaar, Belgium). Sections were taken at 35 μm intervals and a stack of 939 slices was used to digitize the maxilla. These slices were used for generating the surfaces and interfaces of the maxillary bone, PDL, and teeth using in-house software and available general purpose CAD software (Rhinoceros 3D for Windows, Robert McNeel and Associates, Seattle, Washington USA). The foregoing created seven matching bodies; one representing the alveolar bone and the other six were paired as molars and their PDLs. The bodies were in contact along the entire anatomical junction. For reasons of computational efficiency, the bone was represented as a solid volume and the pulp chamber removed. The maximum deviation between the original CT image and reconstructed surface solids was less than 0.5 per cent. The resulting geometric assemblies were imported into general purpose FE analysis software (Cosmos DesignStar, Structural Research and Analysis Corporation, Los Angeles, California, USA) and investigated using linear static analyses. Parabolic tetrahedral elements (15 804) with an average size of 0.3 mm were used for meshing the models. Such elements are more mathematically accurate and are recommended in biomechanical modelling (Remmler *et al.*, 1998).

Material properties. Due to the complexity of biological models, a compromise between the level of detail of the shape and the materials must be reached. Experimental data have shown that two out of three directions of a bone's mechanical properties are almost constant (Hart *et al.*, 1992; Cowin, 2001) and that physiological loading can be prescribed by linear elastic equations (Vollmer *et al.*, 2000; Cowin, 2001); specimen shape and regional variation in bone thickness which are accurately represented in the present model have been shown to condition the nature of the strain gradient (Daegling and Hylander, 1998). For the

present analysis, owing to the dense nature and structure of alveolar bone in the rat and the relatively young age of the animals, the components were modelled as uniform solids (without a cancellous structure) and their mechanical properties taken from Kawarizadeh *et al.* (2003), including a non-linear stress–strain relationship for modelling the PDL.

Load. Three different loading conditions were used. (1) A masticatory load by applying an arbitrary force of 2 N to the occlusal surfaces of the molars. (2) An orthodontic load as applied *in vivo*; a force of 0.2 N was applied to the lingual aspects of the molars in a buccal direction, parallel with the occlusal plane. (3) A combined load with the teeth loaded simultaneously by the occlusal and orthodontic forces. To reproduce the biological constraint as precisely as possible, the model was rigidly restrained along the distal surface of the bony segment and the zygomatic process of the maxilla.

Assessment. In the present study, von Mises stresses were used for comparing the shape response since by measuring the distortion energy, it provides both a value of the stress state and highlights potential areas of bone remodelling (Paynten *et al.*, 1998). This was complemented by the distribution of principal stresses (tensile and compressive) for a better understanding of the mechanical environment induced by the orthodontic appliance. In both cases, the readings ignored the areas close to the restraining points, as these values are artificial and constraint induced.

Results

The appliance appeared to be well tolerated, although initially there was a failure of the animals in both the experimental and sham-treated groups to gain weight compared with the controls; the weight loss, however, was restored by day 4 (data not shown). Of the 62 springs placed, there were just two failures. The expansile force of 0.2 N produced an increase in the intermolar width averaging 0.25 mm by day 2, which had increased to 0.5 mm by day 8 (Figure 1B); whether this was due to compression of the PDL, resorption and/or deformation of alveolar bone, or expansion of the palatal sutures is unclear.

Histology

Unlike human teeth which exhibit physiological mesial drift, rat molars drift distally and the distal alveolar walls are characterized by resorption. The interradicular bone is of the woven or cancellous type composed of osseous trabeculae enclosing a network of vascular channels, some of which are continuous with the PDL; there is no distinct lamina dura. Because of the small size of the jaws, secondary

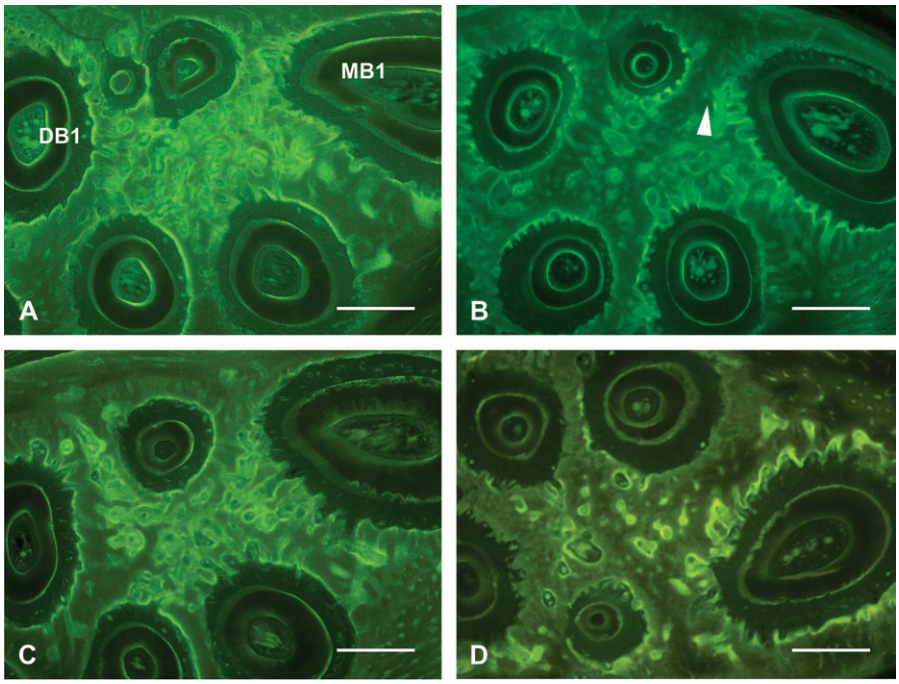

Figure 2 Representative images of the interradicular bone of M1 at the level of the middle third of the roots. The first molar has three buccal and two palatal roots, although accessory roots are common in rat molars. MB1, mesio-buccal root; DB1, disto-buccal root. Each animal received a subcutaneous injection of tetracycline 24 hours prior to sacrifice. (A) 4-day control (B) 4-day experimental. Arrow shows the direction of the applied force. (C) 8-day control. (D) 8-day experimental rat. Bar = 500 μm. Unstained ground sections viewed under ultraviolet light.

osteons are absent and marrow spaces are usually limited to the bone at the level of the apical third of the roots. Bone turnover is rapid; the duration of each remodelling cycle in the alveolar bone of the mandible in adult rats has been estimated at about 6 days (Vignery and Baron, 1980).

The uptake of tetracycline in the control rats suggested a rapid turnover of bone in both the interradicular domain and at the bone–PDL interface and further highlighted individual variation in the remodelling activity of alveolar bone (Figure 2A,C). In the experimental group on the other hand, the incorporation of tetracycline into the interradicular domain appeared to be much reduced, even after 4 days, suggesting that the presence of an orthodontic appliance had resulted in a decline in the rate of bone turnover (Figure 2B,D).

Conventional histology showed that in the experimental group, the applied force resulted in a decrease in the width of the PDL space on the buccal side with foci of hyalinization and loss of normal tissue architecture on the compression side, particularly involving the mesio- and disto-buccal roots of the first molar (Figure 3B). The most significant change, however, was in the appearance of the interradicular bone where there was clear evidence of bone loss and osteopenia; by day 8, the bone was highly trabeculated (Figure 3B–D). This was particularly noticeable at the PDL–bone interface where there were numerous vascular communications with the PDL. The interradicular bone was clearly demarcated from the buccal and lingual alveolar plates of the alveolus composed of lamella bone; any hyalinized PDL tissue had also been eliminated by day 8 (Figure 3C,D). The osseous changes observed in the sham-treated animals were similar to those of the experimental group, the interradicular bone becoming increasingly porous and trabeculated over the 8-day time course (Figure 4). However, at no time was any histological evidence observed suggesting that the annealed springs had produced any tooth movement; the PDL space remained uniform in width with no signs of compression or hyalinization of the periodontal tissues.

Serum ALP and ACP levels

Serum ALP activity was found to have decreased significantly in both the experimental (by day 8) and sham (by day 4) groups compared with the zero-day controls

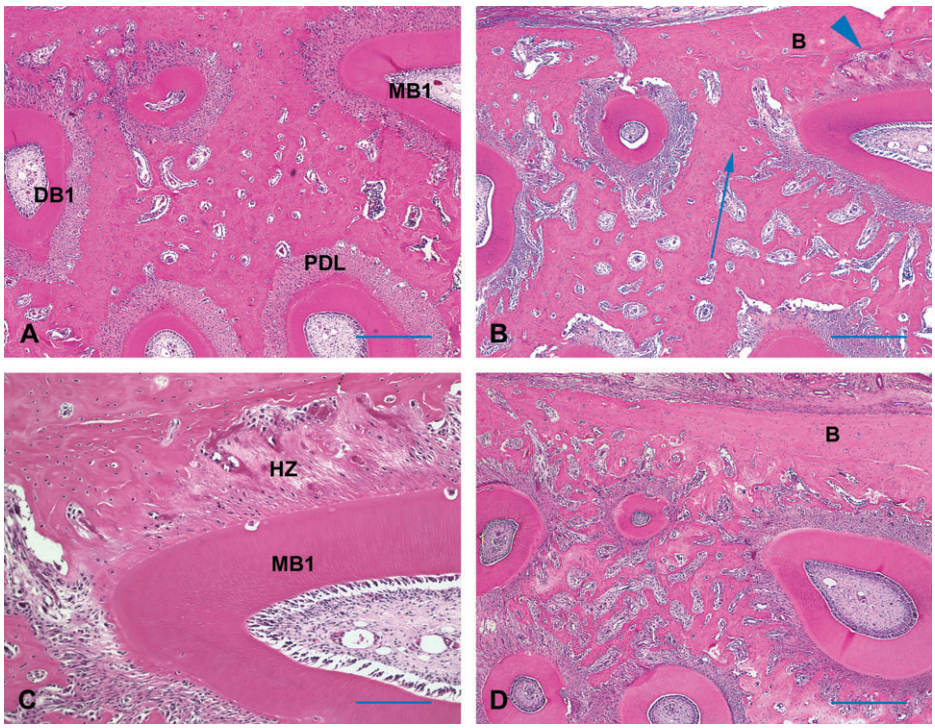

Figure 3 Representative images of the interradicular bone of M1 at the level of the middle third of the roots. MB1, mesio-buccal root; DB1, disto-buccal root; PDL, periodontal ligament; B, buccal alveolar plate. (A) Zero-day control. Alveolar bone in the rat is of the woven type containing a network of vascular channels continuous with the PDL; the bone lacks secondary osteones and, at this level, marrow spaces and there is no distinct lamina dura. Bar = 500 μm. (B) 4-day experimental rat; the bone appears more trabeculated and porotic. Arrow indicates the direction of the applied force. Arrowhead indicates hyalinized tissue. Bar = 500 μm. (C) Detail of hyalinized zone (HZ) within the PDL. Bar = 250 μm. (D) 8-day experimental rat showing further evidence of resorptive remodelling; the interradicular bone is highly trabeculated with numerous vascular communications with the PDL and is clearly distinguishable from the buccal plate. Bar = 500 μm. All sections stained with haematoxylin and eosin.

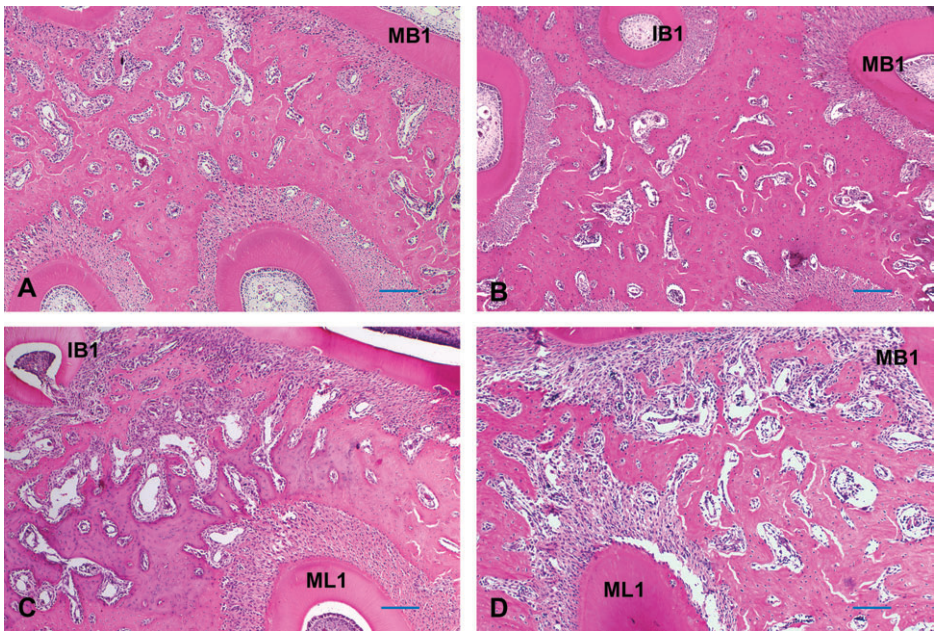

Figure 4 Representative images of the interradicular bone of M1 at the level of the middle third of the roots. MB1, mesio-buccal root; IB1, intermediate buccal root; ML1, mesio-lingual root (A, B) Zero-day controls from different rats showing variation in the morphology of the bone. (C) 4-day sham-treated rat (with an inactivated spring) and (D) 8-day sham-treated rat; both show increased trabeculation of the bone, particularly at the bone–periodontal ligament interface. Bar = 500 μm; sections stained with haematoxylin and eosin.

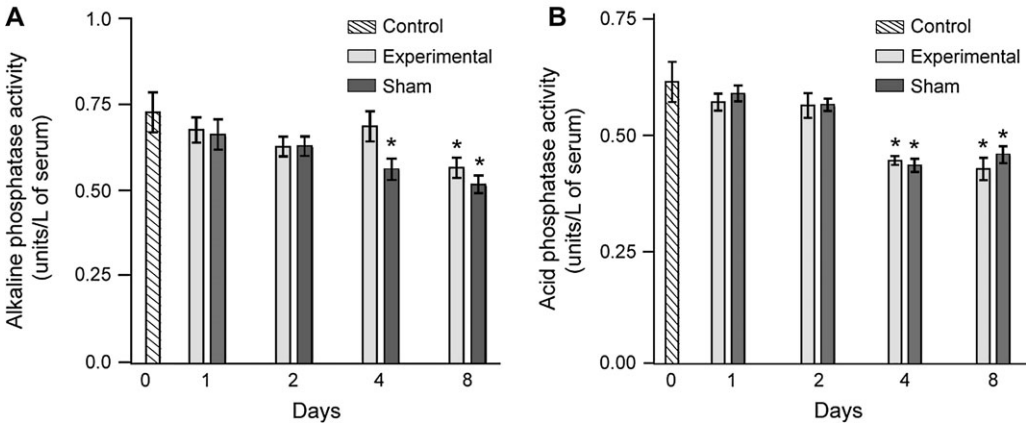

Figure 5 Alkaline (ALP) and acid phosphatase (ACP) activity in serum ($n = 5$) from zero-day controls, experimental (with activated springs), and sham-treated (with passive springs) groups. Samples were assayed in triplicate colormetrically using *p*-nitrophenol phosphate as substrate. *ALP significantly less than zero-day controls. $P < 0.05$. ALP activity was also significantly reduced in the sham-treated animals compared with the experimental group at day 4. **ACP significantly less than zero-day controls. $P < 0.05$.

(Figure 5). Serum ACP activity also showed a significant reduction in both the sham and experimental groups compared with the controls at days 4 and 8 (Figure 5). The only time point at which there was a significant difference between the experimental and sham groups was for ALP at day 4. Measurements of IL-1β levels in the serum by an ELISA were found to be at the detection limit of the assay, and no significant differences in IL-6 were detected between the groups at any point in the timescale (Table 1).

FE analysis

According to the mechanostat theory, the loss of alveolar bone suggested a reduction in functional loading, raising the possibility of stress shielding. To resolve this question, 3D FE analysis of the stresses generated in the alveolar bone following occlusal and orthodontic loading was carried out. The results showed a clear distinction in the biomechanical response of the bone under different loading. For the

occlusal load (mastication), the distortion energy (von Mises stresses) was spread throughout the entire alveolar process affecting the buccal and lingual plates as well as the interradicular bone (Figure 6A). During orthodontic loading, the distortion energy in the bone was significantly less, mechanical unloading being greatest on the interradicular bone and the buccal plates (Figure 6B). Combined loading (Figure 6C) showed a distribution of the distortion energy comparable with the occlusal load, with slightly higher absolute values. Notably, the peak stress areas did not change between the two loading regimens. Figure 7 shows the principal stress distribution (tension and compression) with and without the ligament in the orthodontically loaded bone. The buffering effect of the PDL can be clearly seen (Figure 7A,B), and the bone experiences a complex stress state with a mosaic pattern of interwoven areas of tension (Figure 7C) and compression (Figure 7D).

Table 1 Interleukin-6 (IL-6) levels in serum samples from zero-day controls, experimental, and sham-treated rats.

	Experimental		Sham	
	ng/ml	SEM	ng/ml	SEM
Day 0			297.0	151.5
Day 1	524.0	153.8	238.6	52.6
Day 2	676.8	88.6	559.3	342.0
Day 4	505.5	258.1	953.6	322.2
Day 8	202.3	202.3	393.3	199.4

IL-6 levels in serum were measured by an enzyme-linked immunosorbent assays specific for the rat protein. Data is expressed as mean ± standard error of the mean (SEM) of the mean for three samples assayed in triplicate.

Discussion

The mechanobiology of bone, and particularly alveolar bone, is poorly understood and the findings of this study are counterintuitive. It has been an article of faith, based on a rather liberal interpretation of Wölff's law dating back to Angle (1907), that orthodontic appliances have a

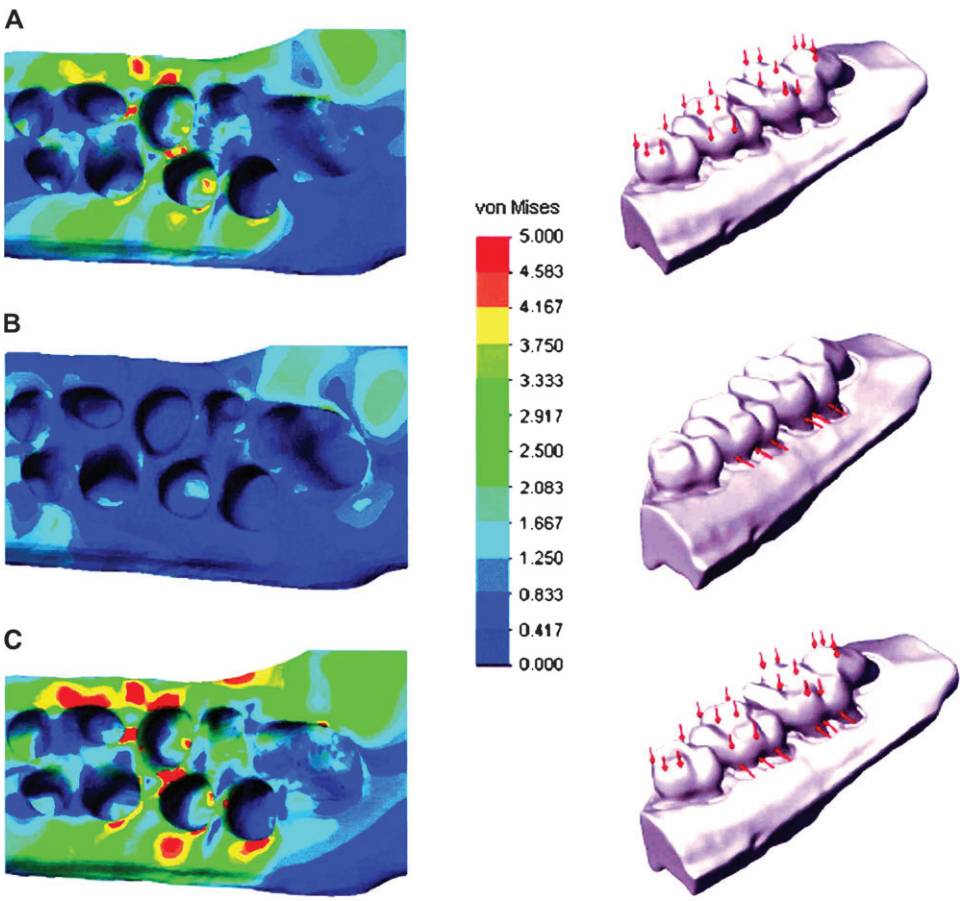

Figure 6 Plots showing the distribution of von Mises stresses (MPa) in alveolar bone during (A) masticatory, (B) orthodontic, and (C) combined masticatory and occlusal loading. Note the similar pattern generated by occlusal (A) and combined loading (C) in marked contrast to the orthodontic load with little or no stress in comparable regions of the bone.

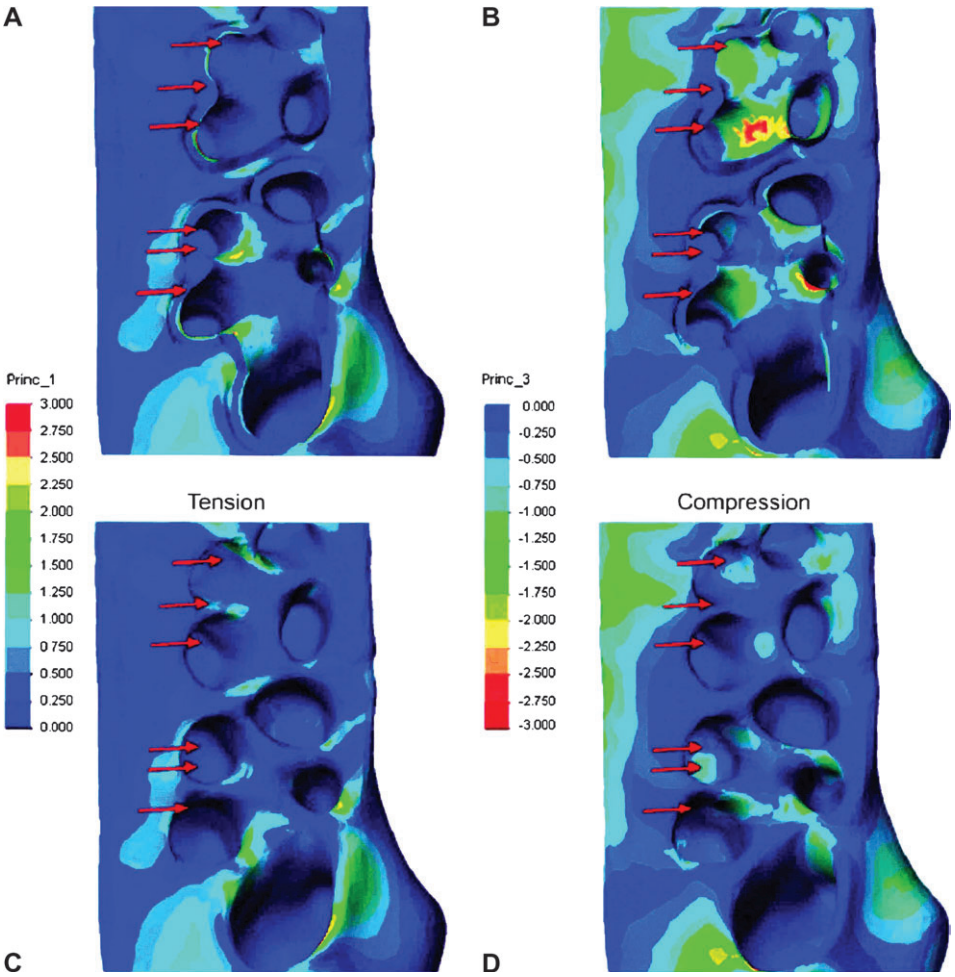

Figure 7 Plots showing the distribution of principal stresses (MPa) in the orthodontically loaded bone illustrating the tension/compression inside the bone and the effect of the periodontal ligament (A and B) on buffering the stresses transmitted to the bone (C and D).

positive effect on bone mass. The findings of the present study indicate otherwise. They suggest that the presence of an orthodontic appliance produces stress shielding of the interradicular bone, leading to osteopenia similar to that associated with prolonged bed rest and spaceflight or the implantation of any rigid metallic device into bone. These observations are also consistent with the findings of experimental masticatory hypofunction in rats, showing that reduced occlusal loading leads to a reduction in alveolar bone mass and bone mineral density (Bresin *et al.*, 1999; Mavropoulos *et al.*, 2004; Kunii *et al.*, 2008).

In the first experimental series, the effects of activated springs were compared with negative controls and, with the benefit of hindsight, the second experimental series could have been improved by including negative as well as positive controls. However, the original intention was to study changes in the PDL at the molecular level and although zero-time negative controls were included, rats with inactivated springs (sham treated) were used to control for the appliance itself. It was not until the serum data was analyzed that it was discovered that the biochemical markers of bone metabolism were essentially the same in both the experimental and sham-treated animals. Nevertheless, given the short timescale of the experiments and the magnitude of the observed changes, it is considered that the findings are valid and sufficiently novel to be reported.

Attempts to quantitate differences in the amount of interradicular bone by measuring bone volume as a percentage of the tissue volume (BV/TV) in a given field proved to be unsatisfactory, using both conventional histology and 3D micro-CT scanning. The considerable variation in BV/TV, depending on the root level at which the section was taken, plus variation in the distribution of the bone itself within the interradicular domain, made sampling difficult and prone to subjective bias. In any event, quantitative histomorphometry cannot tell us whether the loss of bone resulted from a decrease in bone formation and/or an increase in bone

resorption. A surrogate measure of bone turnover was therefore chosen—serum phosphatase levels.

Biochemical markers of bone metabolism such as ALP and ACP levels in serum are frequently employed as adjuncts to bone mass measurements to detect systemic changes of bone turnover in metabolic bone diseases. Even though serum ALP consists of several isoforms that originate from various tissues such as bone, liver, and kidney, it is commonly used as a clinical marker for measuring osteoblast activity and bone formation (Alvarez *et al.*, 1995). The decrease in serum ALP activity detected in both the experimental and sham-treated animals compared with the zero-day controls was consistent with the reduction in bone mass observed histologically and resembled the findings of hindlimb suspension experiments in rats, showing that reduced mechanical loading resulted in decreased bone formation (Morey-Holton and Globus, 1998; Dehority *et al.*, 1999). Since serum markers of bone metabolism reflect whole-body rates of bone formation and resorption, the loss of alveolar bone was clearly of rapid onset, resulting in significant osteopenia after just 2–4 days. Evidence from microgravity studies suggests that in addition to reduced osteoblast differentiation and function (Ontiveros and McCabe, 2003; Zayzafoon *et al.*, 2004), osteoblast apoptosis (Bucaro *et al.*, 2004) may have contributed to the osteopenia, although more recently, Bucaro *et al.* (2007) reported that the effect of microgravity on osteoblasts was independent of the induction of apoptosis.

The decrease in serum ACP activity is more difficult to explain. It suggests that bone resorption had also declined, which is in contrast to post-menopausal and age-related osteoporoses where bone resorption exceeds bone formation (Raisz, 2005). However, whereas osteoporosis is a disease, osteopenia is a physical sign reflecting a reduction in bone mass. Normally, a balance exists between the amount of bone resorbed by osteoclasts and the amount formed by osteoblasts to maintain a constant bone mass; in other words, bone resorption and formation are said to be coupled. The reduction in serum ACP may therefore be a reflection of the fact that bone formation and resorption, although both down-regulated by reduced mechanical loading, remained coupled, the outcome being a localized negative skeletal balance and osteopenia of the tooth-supporting bone. Nevertheless, confirmation of this observation will require future assays of serum for the tartrate-resistant ACP 5b isoform, a unique bone resorption marker released from resorbing osteoclasts (Janckila *et al.*, 2001).

A model that is frequently used to study tissue reaction to orthodontic loading involves mesial movement of the maxillary first molar of the rat with a calibrated coil spring attached to the incisor teeth (King *et al.*, 1991; Verna *et al.*, 1999; Kawarizadeh *et al.*, 2004). Of these studies, only Verna *et al.* (1999) reported alterations in the remodelling activity of the interradicular bone, and, in common with the present investigation, the tissue blocks were sectioned horizontally. However, the load of 0.5 N applied to a single tooth was likely to have been damaging to the tissues, inducing as they suggested, a regional acceleratory phenomenon—an osseous response similar to that occurring during fracture healing and other forms of traumatic bone injury. This is an unlikely explanation for the osteoporosity of the bone observed in the present investigation.

The FE method has been widely used in tooth movement studies and has been shown to be a powerful tool for analyzing the stresses and strains generated in the tissues of the periodontium under various loading conditions (Middleton *et al.*, 1996; Bourauel *et al.*, 2000; Jones *et al.*, 2001; Kawarizadeh *et al.*, 2003, 2004; Toms and Eberhardt, 2003; Cattaneo *et al.*, 2005). FE analyses of orthodontic loading in the rat have shown high strain levels in the PDL and low strains in the bone (Bourauel *et al.*, 2000; Kawarizadeh *et al.*, 2004). Indeed, FE analyses conducted on human models have shown that the maximum strains recorded in the PDL were 35 times higher than for the surrounding alveolar bone (Middleton *et al.*, 1996; Jones *et al.*, 2001). These findings are supported by the present investigation and emphasize the buffering role of the PDL, an effect most likely to be due to a combination of a low modulus of elasticity and high anatomical thickness. The PDL has evolved not only to provide tooth support but also to act as a shock absorber protecting the underlying bone from excessive occlusal loading.

The difference in the distribution of the distortion energy created during biting and orthodontic loading can be explained by the relationship between bone shape and the direction of the load. During mastication, the load acts in an axial direction, thus ‘bending’ the bone in an occluso-apical direction. This is reflected in the morphology of the alveolar process and the buccal and lingual plates, as well as the interradicular bone, can be regarded as a set of three parallel beams. As such, the bone will oppose the occlusal load by its thicker cross section. An orthodontic load tends to bend the bone in a linguo-buccal direction, directing the force against the thinner sections of the beam arrangement, thereby creating tension on the surface of the buccal plate and compression on the lingual plate (Figure 7).

FE analysis showed that the orthodontic force creates a particular constant loading condition in which some areas are shielded from mechanical stress. Moreover, areas of low mechanical stimulation were coincident with sites of bone loss observed histologically, while bone mass was preserved in areas with higher levels of loading. These findings suggest that the mechanostat model can be employed to explain, at least in part, the response of the bone to orthodontic loading. From a mechanical point of view, the orthodontic force disrupts the homeostatic balance of the alveolar bone and creates competition between the mechanical stimuli that will govern the bone’s adaptive reactions. While in terms of absolute value, the masticatory load is far greater than the orthodontic load, it acts intermittently, and its effect on the

bone appears to be muted by the damping effect of the PDL and the continuous action of the orthodontic load. Based on the limited biochemical, histological, and mechanical data of this study, it can be suggested that the presence of an orthodontic appliance changes the dynamics of the stimuli which are received by the bone, the immediate effect being an 'unloading' effect rather than 'directional' loading as expected.

Conclusions

This preliminary investigation has highlighted the importance of having positive as well as negative controls in tooth movement studies. Without a sham-treated group to control for the effect of the orthodontic appliance itself, it might have been concluded that all the osseous changes had resulted from its activation.

It is postulated that in accordance with the mechanostat theory, the most plausible explanation for the osteopenia was stress shielding of the interradicular bone by the appliance, comparable with the disuse atrophy associated with the implantation of rigid metallic devices in orthopaedic surgery—the outcome being a reduction in mechanical loading below the critical threshold required to maintain normal osseous architecture. Nevertheless, it will be important to confirm whether stress shielding of alveolar bone occurs in other currently used experimental models of tooth movement as well as in patients undergoing orthodontic treatment and/or fixed forms of retention.

Address for correspondence

Professor Murray C. Meikle
Faculty of Dentistry
National University of Singapore
5 Lower Kent Ridge Road
Singapore 119074
E-mail: pndmcm@nus.edu.sg

Funding

New Zealand Dental Association Research Foundation; the New Zealand Association of Orthodontists; University of Otago Research Committee; the Academic Research Fund of the National University of Singapore (R222-000-029-112).

Acknowledgements

We wish to thank John Schofield, Lesley Schofield, David Matthews, and the staff of the Hercus Taieri Resource Unit, University of Otago Medical School for their advice and expert management of the animals. We also wish to thank Dr Qing Li, School of Aerospace, Mechanical and Mechatronic Engineering at the University of Sydney for providing access to the analysis software.

References

Alvarez L *et al.* 1995 Discriminative value of biochemical markers of bone turnover in assessing the activity of Paget's disease. Journal of Bone and Mineral Research 10: 458–465

Angle E H 1907 Treatment of malocclusion of the teeth. S S White Manufacturing Co., Philadelphia

Bourauel C, Vollmer D, Jäger A 2000 Application of bone remodeling theories in the simulation of orthodontic tooth movements. Journal of Orofacial Orthopaedics 61: 266–279

Bresin A, Kiliaridis S, Strid K-G 1999 Effect of masticatory function on the internal bone structure in the mandible of the growing rat. European Journal of Oral Sciences 107: 35–44

Bucaro M A *et al.* 2004 Bone survival in microgravity: evidence that modeled microgravity increases osteoblast sensitivity to apoptogens. Annals of the New York Academy of Sciences 1027: 64–73

Bucaro M A *et al.* 2007 The effect of simulated microgravity on osteoblasts is independent of the induction of apoptosis. Journal of Cellular Biochemistry 102: 483–495

Cattaneo P M, Dalstra M, Melsen B 2005 The finite element method: a tool to study orthodontic tooth movement. Journal of Dental Research 84: 428–433

Chow J W M, Wilson A J, Chambers T J, Fox S W 1998 Mechanical loading stimulates bone formation by reactivation of bone lining cells in 13-week-old rats. Journal of Bone and Mineral Research 13: 1760–1767

Cowin S C 2001 Bone mechanics handbook. CRC Press, Boca Raton

Daegling D J, Hylander W L 1998 Biomechanics of torsion in the human mandible. American Journal of Physical Anthropology 105: 73–87

Dehority W *et al.* 1999 Bone and hormonal changes induced by skeletal unloading in the mature male rat. American Journal of Physiology Endocrinology and Metabolism 276: E62–E69

Donaldson C L, Hulley S B, Vogel J M, Hattner J H, Bayers R S, McMillian D E 1970 Effects of prolonged bed rest on bone mineral. Metabolism 19: 1071–1084

Frost H M 1987 Bone 'mass' and the 'mechanostat': a proposal. Anatomical Record 219: 1–9

Glassman A H, Bobyn J D, Tanzer M 2006 New femoral designs: do they influence stress shielding? Clinical Orthopaedics and Related Research 453: 64–74

Hart R T, Hennebel V V, Thongpreda N, van Buskirk W C, Anderson R C 1992 Modeling the biomechanics of the mandible: a three-dimensional finite element study. Journal of Biomechanics 25: 261–286

Huiskes R, Weinans H, van Rietbergen B 1992 The relationship between stress shielding and bone resorption around total hip stems and the effects of flexible materials. Clinical Orthopaedics and Related Research 274: 124–134

Jacobson P C, Beaver W, Grubbs S A, Taft T N, Talmage R V 1984 Bone density in women: college athletes and older athletic women. Journal of Orthopedic Research 2: 328–332

Janckila A J, Takahashi K, Sun S Z, Yam L T 2001 Tartrate-resistant acid phosphatase isoform 5b as serum marker for osteoclast activity. Clinical Chemistry 47: 74–80

Jee W S S, Wronski T J, Morey T J, Kimmel D B 1983 Effects of spaceflight on trabecular bone in rats. American Journal of Physiology 244: R310–R314

Jones M L, Hickman J, Middleton J, Knox J, Volp C A 2001 Validated finite element method study of orthodontic tooth movement in the human subject. Journal of Orthodontics 28: 29–38

Kawarizadeh A, Bourauel C, Jäger A 2003 Experimental and numerical determination of initial tooth mobility and material properties of the periodontal ligament in rat molar specimens. European Journal of Orthodontics 25: 569–578

Kawarizadeh A, Bourauel C, Zhang D, Götz W, Jäger A 2004 Correlation of stress and strain profiles and the distribution of osteoclastic cells induced by orthodontic loading in rat. European Journal of Oral Sciences 112: 140–147

King G J, Keeling S D, McCoy E A, Ward T H 1991 Measuring dental drift and orthodontic tooth movement in response to various initial forces in adult rats. American Journal of Orthodontics and Dentofacial Orthopedics 99: 456–465

Kunii R, Yamaguchi M, Aoki Y, Watanabe A, Kasai K 2008 Effects of experimental occlusal hypofunction and its recovery on mandibular bone mineral density in rats. European Journal of Orthodontics 30: 52–56

Lanyon L E, Baggott D G 1976 Mechanical function as an influence on the structure and form of bone. Journal of Bone and Joint Surgery 58B: 436–443

Mavropoulos A, Kiliaridis S, Bresin A, Amman P 2004 Effect of different masticatory functional and mechanical demands on the structural adaptation of the mandibular alveolar bone in young growing rats. Bone 35: 191–197

Meikle M C 2006 The tissue, cellular, and molecular regulation of orthodontic tooth movement: 100 years after Carl Sandstedt. European Journal of Orthodontics 28: 221–240

Melsen B 1999 Biological reaction of alveolar bone to orthodontic tooth movement. Angle Orthodontist 69: 151–158

Melsen B 2001 Tissue reaction to orthodontic tooth movement—a new paradigm. European Journal of Orthodontics 23: 671–681

Middleton J, Jones M L, Wilson A 1996 The role of the periodontal ligament in bone modeling: the initial development of a time-dependent finite element model. American Journal of Orthodontics and Dentofacial Orthopedics 109: 155–162

Morey-Holton E R, Globus R K 1998 Hindlimb unloading of growing rats: a model for predicting skeletal changes during space flight. Bone 22: 83S–88S

Nilsson B E, Westlin N E 1971 Bone density in athletes. Clinical Orthopaedics and Related Research 77: 179–182

Ontiveros C, McCabe L R 2003 Simulated microgravity suppresses osteoblast phenotype, Runx2 levels and AP-1 transactivation. Journal of Cellular Biochemistry 88: 427–437

Pavlin D, Zadro R, Gluhak-Heinrich J 2001 Temporal pattern of osteoblast-associated genes during mechanically-induced osteogenesis *in vivo*: early responses of osteocalcin and type I collagen. Connective Tissue Research 42: 135–148

Paynten W M, Ben-Nissan B, Mercer D J 1998 Optimal topology design using a global self-organizational approach. International Journal of Solid Structures 35: 219–237

Raisz L G 2005 Pathogenesis of osteoporosis: concepts, conflicts, and prospects. Journal of Clinical Investigation 115: 3318–3325

Remmler D, Olson L, Duke D, Skstrom R, Matthews D, Ullrich C 1998 Presurgical finite element analysis from routine computed tomography studies for craniofacial distraction. II. An engineering model for gradual correction of asymmetric skull deformities. Plastic and Reconstructive Surgery 102: 1395–1404

Skerry T M 2006 One mechanostat or many? Modifications of the site-specific response of bone to mechanical loading by nature and nurture. Journal of Musculoskeletal and Neurological Interactions 6: 122–127

Toms S R, Eberhardt A W 2003 A nonlinear finite element analysis of the periodontal ligament under orthodontic tooth loading. American Journal of Orthodontics and Dentofacial Orthopedics 123: 657–665

Verna C, Zaffe D, Siciliani G 1999 Histomorphometric study of bone reactions during orthodontic tooth movement in the rat. Bone 24: 371–379

Verna C, Dalstra M, Lee T C, Cattaneo P M, Melsen B 2004 Microcracks in the alveolar bone following orthodontic tooth movement: a morphological and morphometric study. European Journal of Orthodontics 26: 459–467

Vignery A, Baron R 1980 Dynamic histomorphometry of alveolar bone remodeling in the adult rat. Anatomical Record 196: 191–200

Vollmer D, Meyer U, Joos U, Vegh A, Piffko J 2000 Experimental and finite element study of a human mandible. Journal of Cranio-Maxillo-Facial Surgery 28: 91–96

Zayzafoon M, Gathings W E, McDonald J M 2004 Modeled microgravity inhibits osteogenic differentiation of human mesenchymal stem cells and increases adipogenesis. Endocrinology 145: 2421–2432